Binding Modes of μ-Conotoxin to the Bacterial Sodium Channel (Na_VAb)

Rong Chen* and Shin-Ho Chung
Computational Biophysics Group, Research School of Biology, Australian National University, Canberra, Australia

ABSTRACT Polypeptide toxins isolated from the venom of cone snails, known as μ-conotoxins, block voltage-gated sodium channels by physically occluding the ion-conducting pathway. Using molecular dynamics, we show that one subtype of μ-conotoxins, PIIIA, effectively blocks the bacterial voltage-gated sodium channel Na_VAb, whose crystal structure has recently been elucidated. The spherically shaped toxin, carrying a net charge of $+6$ *e* with six basic residues protruding from its surface, is attracted by the negatively charged residues on the vestibular wall and the selectivity filter of the channel. The side chain of each of these six arginine and lysine residues can wedge into the selectivity filter, whereas the side chains of other basic residues form electrostatic complexes with two acidic residues on the channel. We construct the profile of potential of mean force for the unbinding of PIIIA from the channel, and predict that PIIIA blocks the bacterial sodium channel with subnanomolar affinity.

INTRODUCTION

Voltage-gated sodium channels (Na_V), responsible for the rising phase of action potential, are ubiquitous in muscle and neuronal cells of mammals. To date, nine channel isoforms of the Na_V1 subfamily have been identified, which have similar functional properties but different distribution in muscle and nerve cells (1). Na_V channels have also been discovered in bacteria (2,3). The crystal structure of the Na_V channel from *Arcobacter butzleri* (Na_VAb) shows that the channel is a homotetramer, and each monomer consists of six transmembrane helices S1–S6 (4). The four helices S1–S4 form the voltage-sensing domain, whereas the S5–S6 helices form the pore domain, similar to that of voltage-gated potassium (Kv) channels (5). Mammalian Na_V channels, on the other hand, are composed of four nonidentical subunits, each subunit consisting of six transmembrane helices (6).

Numerous molecules, ranging from small synthetic compounds to large polypeptide toxins, which interfere with the conductance properties of Na_V channels, have been identified. The toxins and drugs bind to various parts of the channel complex; for example, some of these molecules, such as tetrodotoxin, saxitoxin, and μ-conotoxin, wedge into the selectivity filter of the channel and occlude the ion-conducting conduit (6,7), whereas certain scorpion toxins bind to the voltage-sensing domain and interfere with the gating kinetics of the channel (8,9). These toxins are useful tools for probing the structure and physiological roles of Na_V channels (10), and provide templates for developing pharmaceutical agents. For example, μ-conotoxins are believed to be potential leads for developing novel analgesics (11,12).

Polypeptide μ-conotoxins, isolated from the venom of cone snails, can bind to Na_V channels and occlude the ion-conducting pathway with the side chain of an arginine or lysine residue. μ-Conotoxins typically contain 22–25 amino acids, with six cysteine residues forming three disulfide bridges arranged in a class III frame work (13). Specifically, no residue is present between the first and the second cysteine residues, or between the fifth and the sixth cysteine residues. In addition, the fourth and fifth cysteine residues are separated by four or five residues. A number of μ-conotoxins of distinct potency and selectivity to Na_V1 channels have been identified. Some of the best studied are GIIIA, PIIIA, and SmIIIA (7). For example, GIIIA, isolated from *Conus geographus*, selectively targets skeletal muscle Na_V channels, with the largest affinity for the $Na_V1.4$ channel (14). PIIIA isolated from *Conus purpurascens* blocks both muscle and neuronal Na_V channels with half-maximal inhibitory concentration (IC_{50}) values in the nanomolar range (14). SmIIIA, isolated from *Conus stercusmuscarum*, selectively targets tetrodotoxin-resistant Na_V channels (15). These toxins block Na_V1 channels in a voltage-dependent manner, with a higher affinity at a more negative membrane potential (16,17). However, the effect of μ-conotoxins on bacterial Na_V channels has not been demonstrated yet. For further details, the reader is referred to several comprehensive reviews on μ-conotoxins (6,7,10,18,19).

Using mutational analysis, a number of studies have identified some key residues of μ-conotoxin that are important in its binding to the Na_V1 channels (16,17,20,21). These studies suggest that all six basic residues of PIIIA may be involved in the toxin binding (17,21), because the substitution of any of these basic residues with a neutral residue reduces the binding affinity by one or two orders of magnitude. Similarly, a single mutation of any basic residue of GIIIA causes the binding affinity of the toxin for rat skeletal muscle Na_V1 channels to decrease by 10- to 100-fold (16). These results are in contrast to that found for the blockers of Kv channels such as charybdotoxin, whose binding affinity has been attributed to only two or three of the seven basic

Submitted November 15, 2011, and accepted for publication December 27, 2011.

*Correspondence: rong.chen@anu.edu.au

Editor: Carmen Domene.

© 2012 by the Biophysical Society

0006-3495/12/02/0483/6 $2.00

doi: 10.1016/j.bpj.2011.12.041

residues in the toxin (22,23). It appears that a single binding mode, which is appropriate for the blockers of Kv channels, is not adequate to explain the available experimental data for PIIIA. For example, in the model proposed by McArthur et al. (21), the residue Arg-14 of PIIIA occludes the channel selectivity filter, with the residue Arg-2 facing water. According to this model, mutations of Arg-2 are not expected to have significant effects on the binding affinity of the toxin. Yet, a 100-fold reduction in the binding affinity of PIIIA was observed when the residue Arg-2 was mutated to an alanine (21).

Here, with molecular dynamics (MD) simulations, we first demonstrate that PIIIA readily blocks the Na_VAb channel. We show that the six basic residues of the toxin are equally likely to protrude into the selectivity filter. We then construct the potential of mean force (PMF) profile for the unbinding of PIIIA along the channel axis, and predict the IC_{50} for the block of PIIIA to Na_VAb.

METHODS

MD simulations

The structures of the Na_VAb channel (PDB ID 3RVY) (4) and PIIIA (PDB ID 1R9I) (24) are obtained from the Protein Data Bank. First, we equilibrate the channel pore domain (residues 105 to 221, see Fig. 1, *A* and *B*), embedded in a 2-oleoyl-1-palmitoyl-*sn*-glycero-3-phosphochlorine bilayer in a 90 × 90 × 110 Å box of TIP3P water with 0.2 M NaCl for 1.5 ns. We then place PIIIA 15 Å above the channel outer vestibule, and subsequently simulate the system three times with each simulation lasting for 10 ns initially. In two of the three simulations, toxin block is observed. These two simulations are extended to 20 or 30 ns.

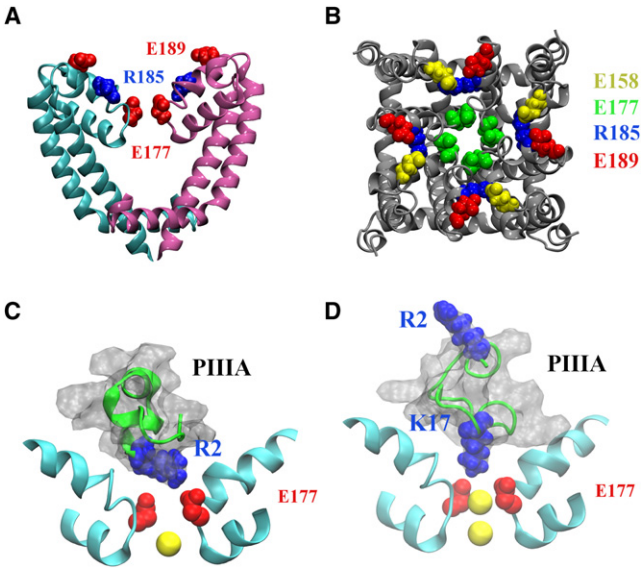

FIGURE 1 Structure of the pore domain of the Na_VAb channel, viewed perpendicular to the channel axis (*A*) and from the periplasmic side of the lipid bilayer along the channel axis (*B*). PIIIA spontaneously blocks the Na_VAb channel with the side chain of the residue Arg-2 (*C*) or Lys-17 (*D*) occluding the selectivity filter within 10 ns. The sodium ion in the selectivity filter is shown as a yellow sphere. In *A*, only two of the four channel subunits (in *cyan* and *pink*) are shown for clarity.

All MD simulations are performed using NAMD 2.8 (25), with periodic boundary conditions, a 2-fs time step at 1 atm and 300 K. The CHARMM36 force field is used to describe the lipids, proteins, and ions (26,27). The switch and cutoff distances for short-range interactions are set to 8.0 Å and 12.0 Å, respectively. The particle mesh Ewald method is used to describe long-range electrostatic interactions, with a maximum grid spacing of 1.0 Å. The SHAKE (28) and SETTLE (29) algorithms are used to keep the bond lengths in the system rigid.

Molecular docking

We use the rigid-body docking program, ZDOCK (30), to explore all the likely binding modes of PIIIA to Na_VAb. For the docking calculations, the channel protein in isolation, not embedded in the lipid bilayer, is used. The toxin is then allowed to dock only to the outer vestibular wall and the selectivity filter. Those channel regions, which are normally buried in the lipid bilayer or exposed to the intracellular space, are made inaccessible to the toxin during docking calculations. Of the 500 docking structures generated, we select the complexes in which one of the basic residues of the toxin is wedged into the selectivity filter. The highest ranked structures among these are then chosen for subsequent MD simulations.

Umbrella sampling

A series of umbrella sampling runs are carried out using umbrella windows placed at 0.5 Å intervals to construct the PMF of the blocker and channel interaction. A force of 20 kcal/mol/Å is applied to pull the toxin out from the binding site along the central z axis of the channel, which is chosen as the reaction coordinate. During the pulling, harmonic restraint is applied to maintain a rigid toxin backbone. The channel backbone atoms are fixed during pulling.

The center of mass (COM) of the toxin backbone is harmonically restrained to the center of each umbrella window using a force constant of 20–30 kcal/mol/Å^2. The COM of the toxin backbone is confined to be within a cylinder of 8 Å in radius centered on the channel axis, using a flat-bottom harmonic restraint (20 kcal/mol/Å^2). The COM of the channel is at $z = 0$ Å. Each umbrella window is simulated for 10–15 ns. A convergence of PMF profiles is assumed if the depth of the PMF profile changes by $<0.5\ kT$ over the last 2 ns. The first 5 ns of each window is considered as equilibration and removed from data analysis. The trajectory data are then analyzed using the weighted histogram analysis method to construct a PMF profile (31). From the PMF profile, an IC_{50} value is calculated using the method described elsewhere (32).

RESULTS AND DISCUSSION

PIIIA blocks Na_VAb spontaneously

PIIIA blocks a wide range of mammalian Na_V channels with nanomolar affinity (14). Here, we demonstrate that PIIIA is also capable of blocking the bacterial Na_VAb channel. The toxin, initially placed 15 Å above the channel outer vestibule, spontaneously binds to the channel and occludes the channel selectivity filter within 10 ns.

To examine the ability of PIIIA in blocking the Na_VAb channel, we perform three independent simulations with different random initial velocities and the same starting configuration. The position from which the toxin is initially released is 15 Å above the position of the toxin when it is

bound to the channel. The COM of the toxin at the bound position and the released site are at $z = 25$ and $z = 40$ Å, respectively. At the release site, the PMF is approximately zero (see Fig. 3). Each simulation is run for 10 ns initially. In the first simulation, the toxin is observed to bind to the channel within 5 ns, with two arginine residues (Arg-14 and Arg-20) attached to two Glu-189 residues of two subunits of the channel. The side chain of the Arg-2 residue then quickly occludes the channel selectivity filter (Fig. 1 *C*). The simulation is extended to 30 ns. The residue Arg-2 continues to occlude the selectivity filter at the end of the simulation, although the toxin reorientates itself such that Arg-12 is attracted to the channel wall with Arg-14 gradually detached. The overall shape of the toxin remains unchanged because of the three disulfide bridges cross-linking its backbone. The root mean-square deviation of the toxin backbone atoms with reference to the starting structure is in the range of between 2.0 and 2.7 Å over the last 5 ns of the 30-ns simulation. In the second simulation, the Arg-14 residue of the toxin attaches to the channel residue Glu-158 rapidly. Then, being firmly bound to the channel, the side chain of the Lys-17 residue gradually wedges into the selectivity filter, occluding the permeation pathway (Fig. 1 *D*). The bound complex remains stable throughout the extended simulation of 20 ns. In the third simulation, the toxin also becomes attached to the channel, but no block is observed. Therefore, the simulation is discontinued at 10 ns. The simulations demonstrate that PIIIA blocks the Na_VAb channel, and suggest that PIIIA may adopt alternative binding modes on block.

Alternative binding modes

In addition to demonstrating the ability of PIIIA to block the Na_VAb channel, the results shown in Fig. 1, *C* and *D*, also suggest that the toxin may be capable of blocking the channel with various binding modes. Here, we explore the possibility that the side chains of four other basic residues of the toxin, in addition to those of Arg-2 and Lys-17, are equally likely to wedge into the selectivity filter of the channel. To test this hypothesis, we dock the side chain of each of these four basic residues, namely, Arg-12, Arg-14, Arg-20, and Lys-9, into the channel selectivity filter, using the molecular docking program ZDOCK (30), and then equilibrate the toxin-channel complex embedded in the same 2-oleoyl-1-palmitoyl-*sn*-glycero-3-phosphochlorine bilayer in a box of water and ions for 10 ns. In each case, we remove one Na^+ ion from the bulk to the selectivity filter. Our MD simulations reveal that the selectivity filter in the absence of any applied electric potential is normally occupied by two Na^+ ions (see also the results of Carnevale et al. (33)). In the presence of a strong applied potential, but in the absence of a blocker, one of the two ions moves out of the selectivity filter, toward the intracellular mouth of the channel, and then another one reenters the filter from the external vestibule (see Fig. S1 in the Supporting Material). We surmise that, in the conducting state of the channel, the selectivity filter will be occupied by the side chain of one of the basic residues of PIIIA and one Na^+ ion. We show that with different residues occluding the channel selectivity filter, the toxin forms similar contacts with the channel.

Table 1 tabulates the key residue pairs formed between the toxin PIIIA and the Na_VAb channel when the channel selectivity filter is occluded by each of the six basic residues of the toxin. The average number of hydrogen bonds formed by each residue pair over a simulation period of 5 ns is also given. Here, a hydrogen bond is considered to be formed if the distance between the donor and acceptor atoms (nitrogen or oxygen) is ≤ 3.0 Å and the donor-hydrogen-acceptor angle is $\geq 150^\circ$ (34). Results displayed in Table 1 show that, with different residues protruding into the channel selectivity filter, two toxin-channel electrostatic contacts are formed at the outer vestibule of the channel. The only exception is Arg-12, the binding of which to the channel selectivity filter only allows one additional contact to be formed at the channel outer vestibule. This is consistent with mutagenesis experiment, which shows that the mutation of Arg-12 to neutral amino acids causes the least reduction in binding affinity (21). The bound state by PIIIA and the Na_VAb channel with the toxin residue Arg-2 occluding the channel selectivity filter is shown in Fig. 2 *A*. When Arg-2 occludes the channel pore by forming a hydrogen bond with the Glu-177 residue at the entrance of the channel selectivity filter, the toxin forms two additional electrostatic complexes with the channel outer vestibule. Specifically, the residue Arg-12 of the toxin forms nearly two hydrogen bonds with a Glu-189 residue of the channel, whereas the toxin residue Arg-20 forms nearly two hydrogen bonds with the Glu-189 residue of an adjacent subunit of the channel. The lengths of the salt bridges formed by the two residue pairs fluctuate minimally with time (see Fig. S2 in the Supporting Material). Therefore, the toxin is firmly attached to the channel. The bound state by PIIIA and the Na_VAb channel with the toxin residue Lys-9 protruding

TABLE 1 Key residue pairs formed between the toxin PIIIA and the Na_VAb channel when each of the six basic residues of the toxin occludes the channel selectivity filter

Residue in selectivity filter	Toxin-channel interaction pairs		
	First	Second	Third
Arg-2	R2-E177 (1.0)	R12-E189 (1.9)	R20-E189 (1.8)
Lys-9	K9-E177 (1.5)	R2-E158 (1.8)	R14-E189 (1.2)
Arg-12	–	R14-E189 (1.7)	–
Arg-14	R14-S178 (0.8)	R2-E189 (1.7)	R12-E158 (1.7)
Lys-17*	R2-E189 (1.7)	R12-E158 (1.6)	R14-E158 (1.3)
Arg-20	R20-E177 (0.9)	R12-E189 (1.2)	R14-E158 (1.6)

Shown in brackets are the average numbers of hydrogen bonds formed between the residue pairs. Standard errors of means are ~0.05 in all cases.
*Lys-17 forms 0.3 hydrogen bonds with the channel residue Glu-177.

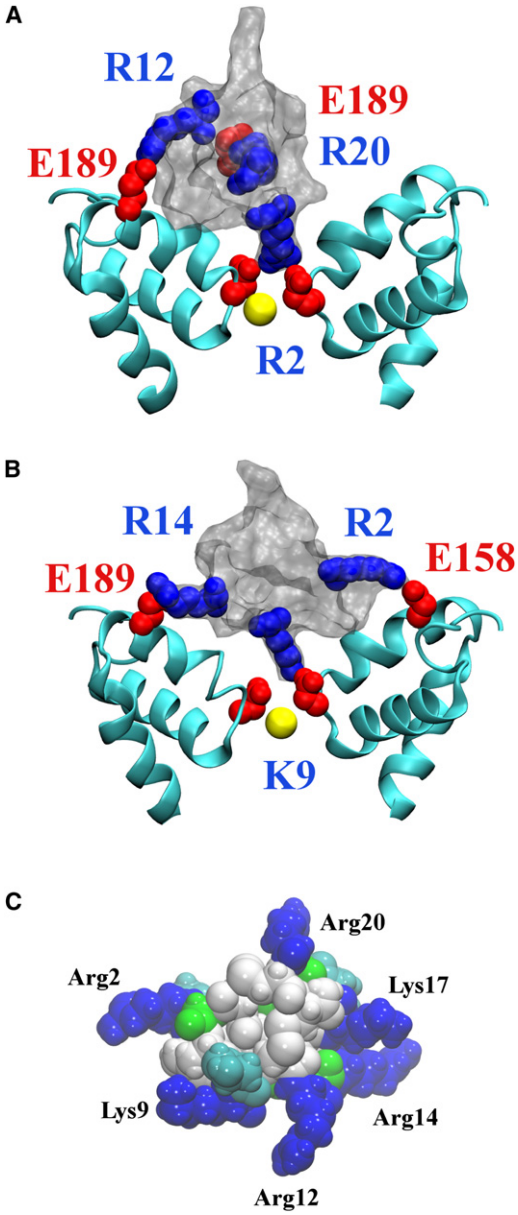

FIGURE 2 Toxin PIIIA occludes the selectivity filter of the Na_VAb channel with the side chain of the residue Arg-2 (*A*) or Lys-9 (*B*). Toxin surface is shown in transparent silver. In *C*, the molecular surface of PIIIA is shown, with the six basic residues colored in blue, polar residues in green, hydrophobic residues in white, and hydroxyproline in cyan.

into the channel selectivity filter is shown in Fig. 2 *B*. When Lys-9 occludes the channel pore, the toxin also forms two additional contacts with the channel outer vestibule: the residues Arg-2 and Arg-14 form electrostatic complexes with the residues Glu-158 and Glu-189 of two opposite subunits of the channel. The salt bridge by Arg-2 is stable, whereas the salt bridge by Arg-14 occasionally breaks, likely due to the electrostatic forces from Glu-158 (Fig. S2). Therefore, the toxin PIIIA can form similar electrostatic complexes with the channel selectivity filter and outer vestibule, suggesting a multiple binding mode mechanism by the toxin.

Recently, McArthur et al. (21) carried out detailed studies on PIIIA binding to rat skeletal muscle Na_V channels. They replaced each of the six basic residues except Lys-9 with a neutral residue and calculated the changes in effective valence, $z\delta$. This quantity expresses, for each mutant, the magnitude of changes in the apparent dissociation constant in response to an applied potential. Their measurements reveal that the change in $z\delta$ value is small when Arg-2 is replaced with alanine, compared with the change in $z\delta$ value when Lys-17 or Arg-14 is replaced with alanine. Because the voltage-dependence of the binding affinity of the mutant toxin differs depending on which basic residue is mutated does not necessarily imply that there is a unique binding mode. Similarly, our claim that the toxin can bind to the channel in different modes is not contradicted by the experimental measurements of McArthur et al. (21).

Structural basis for the multiple binding mode

The μ-conotoxin PIIIA has two key features, which confer its ability to block the Na_VAb channel with alternative binding modes. First, the basic residues of PIIIA are approximately coplanar and symmetrically distributed (Fig. 2 *C*). The symmetry of PIIIA means its ability to form similar electrostatic complexes with the channel outer vestibule when different residues occlude the selectivity filter. In contrast, polypeptide pore blockers of Kv channels are not symmetrical and have well-defined long principal axes, which are approximately perpendicular to the channel axis on toxin binding, limiting the possibilities of alternative binding modes (32). Second, PIIIA does not carry an acidic residue, which is repulsive to the channel outer vestibule rich in acidic residues (Fig. 1 *B*). In addition, the C-terminus of PIIIA is amidated, and is therefore neutral. A predominant binding mode is difficult to achieve without a negative charge, because all the parts of the toxin are equally attractive to the channel outer vestibule. In each of all Kv channel blockers, except margatoxin (35), there is an acidic residue at the opposite side of the key lysine residue whose side chain blocks the selectivity filter. The presence of this acidic residue ensures that the toxin is oriented such that the important lysine residue is pointing the selectivity as it approaches the channel entrance. It is expected that mutating one of the six basic residues to aspartate or glutamate may reduce the number of possible binding modes by PIIIA on blocking a Na_V channel. We note that a number of other μ-conotoxins such as SxIIIA, SxIIIB, and SIIIB also do not carry an acidic residue and are C-terminally amidated (11).

PMF profiles

To determine the potency of the block of PIIIA to the Na_VAb channel, PMF profiles are constructed using umbrella

sampling, where the channel axis is chosen as the reaction coordinate. The starting configurations for each umbrella window are generated by pulling the toxin out from the binding site corresponding to that shown in Fig. 2 *A*, which is predicted from unbiased MD simulations. To examine the effect of ion configurations in the selectivity filter on the binding, we construct the PMF profiles with one or two Na^+ ions in the selectivity filter. To generate the bound state of the two-ion configuration, we move one bulk Na^+ into the inner vestibule of the one-ion bound state and then equilibrate the system for 5 ns. The converged PMF profiles are displayed in Fig. 3. The depth of the PMF profile constructed in the presence of either one or two Na^+ ions in the selectivity filter differs by <2 *kT*, suggesting that the ion configuration of the selectivity filter has minimal effect on the PMF. The IC_{50} value corresponding to the PMF profile of the one-ion configuration is 0.03 nM and the two-ion configuration is 0.1 nM, substantially lower than that determined experimentally for PIIIA on mammalian Na_V channels, which range from 36 nM for $Na_V1.4$ to 3.2 μM for $Na_V1.3$ (36). The discrepancy between our prediction and experiment is not surprising. Bacterial and mammalian Na_V channels differ significantly in both sequence and structure, and this determines the channel's sensitivity to toxins. For example, GIIIA is 20-fold more selective for the rat over the human $Na_V1.4$ channel, which is thought to be due to the difference in only one residue in the channel outer vestibule (37).

To demonstrate the relative probability of the different binding modes shown in Table 1, we also construct the PMF profile for the unbinding of the toxin from the binding mode shown in Fig. 2 *B* predicted from docking calculations. The resulting PMF profile is displayed in Fig. 3. The depth of the PMF profile differs with that obtained for the binding mode of Fig. 2 *A* by only ~1 *kT*, suggesting that the two binding modes predicted from MD simulations and docking calculations encounter similar free energy, and therefore, are equally probable.

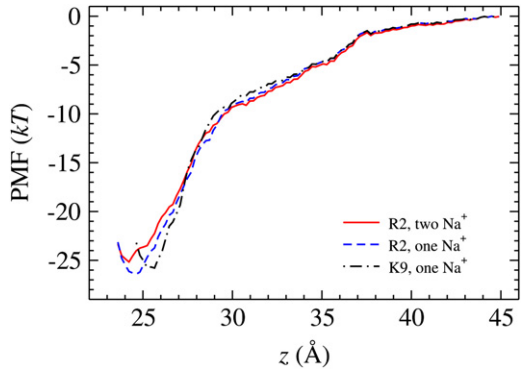

FIGURE 3 PMF profiles for the unbinding of PIIIA from the Na_VAb channel for the two binding modes of Fig. 2, in the presence of one or two Na^+ ions in the selectivity filter.

CONCLUSIONS

Using MD simulations, we demonstrate for the first time, to our knowledge, that the PIIIA blocks the bacterial Na_VAb channel. The toxin, when released in water, spontaneously binds to the channel outer vestibule and occludes the channel selectivity filter with the side chain of an arginine or a lysine residue. We then show that PIIIA can block the channel with each of its six basic residues by forming similar electrostatic contacts with the channel, suggesting that the toxin is capable of blocking Na_VAb, not in one particular mode, but in many different modes. We suggest that the symmetrically distributed basic residues of the toxin largely account for this multiple binding mode mechanism. This postulated binding mode of PIIIA to Na_VAb is unique among all other polypeptide toxins studied thus far. For charybdotoxin or α-kaliotoxin, the side chain of one key lysine residue wedges into the selectivity filter, whereas the oblate body of the toxin is stabilized by one or more salt bridges or hydrogen bonds it forms with the residues on the vestibular wall (32).

The profile of PMF we constructed indicates that PIIIA will block Na_VAb with subnanomolar affinity. Because Na_V Ab is a homotetramer and PIIIA possesses protruding basic side chains at a regular spacing, the channel-toxin complex shows two interacting residue pairs, in addition to a hydrogen bond in the selectivity filter. Because all mammalian voltage-gated sodium channels are composed of four nonidentical subunits, it is conceivable that only one contact is formed between a subtype of μ-conotoxins and the vestibular wall. Thus, PIIIA may block mammalian Na_V channels at relatively low affinity, compared to its affinity to Na_VAb.

To date, several subtypes of μ-conotoxins are the only polypeptide toxins known to block the ion-conducting pathway of the sodium channel. In addition, several synthetic compounds used for local anesthetics have been developed that target the ion-conducting pathway of sodium channels. It will be of interest to elucidate the primary mechanism of action of these small molecules on human sodium channels and compare how it is similar to or different from the way PIIIA interferes with the conduction properties of Na_VAb. Furthermore, the toxin we studied here may be used as a template for designing new classes of agents for combating neuropathic pain.

SUPPORTING MATERIAL

Two figures are available at http://www.biophysj.org/biophysj/supplemental/S0006-3495(11)05472-5.

Molecular graphics are generated using VMD (38). This research was undertaken on the National Computational Infrastructure National Facility in Canberra, Australia, which is supported by the Australian Commonwealth Government. This work is supported by grants from the National Health and Medical Research Council of Australia.

REFERENCES

1. Catterall, W. A., A. L. Goldin, and S. G. Waxman. 2005. International Union of Pharmacology. XLVII. Nomenclature and structure-function relationships of voltage-gated sodium channels. *Pharmacol. Rev.* 57:397–409.
2. Ren, D., B. Navarro, …, D. E. Clapham. 2001. A prokaryotic voltage-gated sodium channel. *Science* 294:2372–2375.
3. Koishi, R., H. Xu, …, D. E. Clapham. 2004. A superfamily of voltage-gated sodium channels in bacteria. *J. Biol. Chem.* 279:9532–9538.
4. Payandeh, J., T. Scheuer, …, W. A. Catterall. 2011. The crystal structure of a voltage-gated sodium channel. *Nature* 475:353–358.
5. Long, S. B., E. B. Campbell, and R. Mackinnon. 2005. Crystal structure of a mammalian voltage-dependent *Shaker* family K^+ channel. *Science* 309:897–903.
6. Catterall, W. A., S. Cestèle, …, T. Scheuer. 2007. Voltage-gated ion channels and gating modifier toxins. *Toxicon* 49:124–141.
7. Al-Sabi, A., J. McArthur, V. Ostroumov, and R. J. French. 2006. Marine toxins that target voltage-gated sodium channels. *Mar. Drugs* 4:157–192.
8. Wang, J. T., V. Yarov-Yarovoy, …, W. A. Catterall. 2011. Mapping the receptor site for α-scorpion toxins on a Na^+ channel voltage sensor. *Proc. Natl. Acad. Sci. USA* 108:15426–15431.
9. Zhang, J. Z., V. Yarov-Yarovoy, …, W. A. Catterall. 2011. Structure-function map of the receptor site for β-scorpion toxins in domain II of voltage-gated sodium channels. *J. Biol. Chem.* 286:33641–33651.
10. Dutertre, S., and R. J. Lewis. 2010. Use of venom peptides to probe ion channel structure and function. *J. Biol. Chem.* 285:13315–13320.
11. Norton, R. S. 2010. μ-Conotoxins as leads in the development of new analgesics. *Molecules* 15:2825–2844.
12. Khoo, K. K., M. J. Wilson, …, R. S. Norton. 2011. Lactam-stabilized helical analogues of the analgesic μ-conotoxin KIIIA. *J. Med. Chem.* 54:7558–7566.
13. Terlau, H., and B. M. Olivera. 2004. *Conus* venoms: a rich source of novel ion channel-targeted peptides. *Physiol. Rev.* 84:41–68.
14. Safo, P., T. Rosenbaum, …, G. Mandel. 2000. Distinction among neuronal subtypes of voltage-activated sodium channels by μ-conotoxin PIIIA. *J. Neurosci.* 20:76–80.
15. West, P. J., G. Bulaj, …, D. Yoshikami. 2002. μ-Conotoxin SmIIIA, a potent inhibitor of tetrodotoxin-resistant sodium channels in amphibian sympathetic and sensory neurons. *Biochemistry* 41:15388–15393.
16. Becker, S., E. Prusak-Sochaczewski, …, R. J. French. 1992. Action of derivatives of μ-conotoxin GIIIA on sodium channels. Single amino acid substitutions in the toxin separately affect association and dissociation rates. *Biochemistry* 31:8229–8238.
17. McArthur, J. R., V. Ostroumov, …, R. J. French. 2010. Multiple, distributed interactions of μ-conotoxin PIIIA associated with broad targeting among voltage-gated sodium channels. *Biochemistry* 50:116–124.
18. Olivera, B. M. 1997. E.E. Just Lecture, 1996. *Conus* venom peptides, receptor and ion channel targets, and drug design: 50 million years of neuropharmacology. *Mol. Biol. Cell* 8:2101–2109.
19. Lewis, R. J., and M. L. Garcia. 2003. Therapeutic potential of venom peptides. *Nat. Rev. Drug Discov.* 2:790–802.
20. Shon, K. J., B. M. Olivera, …, D. Yoshikami. 1998. μ-Conotoxin PIIIA, a new peptide for discriminating among tetrodotoxin-sensitive Na channel subtypes. *J. Neurosci.* 18:4473–4481.
21. McArthur, J. R., G. Singh, …, R. J. French. 2011. Orientation of μ-conotoxin PIIIA in a sodium channel vestibule, based on voltage dependence of its binding. *Mol. Pharmacol.* 80:219–227.
22. Park, C. S., and C. Miller. 1992. Interaction of charybdotoxin with permeant ions inside the pore of a K^+ channel. *Neuron* 9:307–313.
23. Park, C. S., and C. Miller. 1992. Mapping function to structure in a channel-blocking peptide: electrostatic mutants of charybdotoxin. *Biochemistry* 31:7749–7755.
24. Nielsen, K. J., M. Watson, …, R. J. Lewis. 2002. Solution structure of μ-conotoxin PIIIA, a preferential inhibitor of persistent tetrodotoxin-sensitive sodium channels. *J. Biol. Chem.* 277:27247–27255.
25. Phillips, J. C., R. Braun, …, K. Schulten. 2005. Scalable molecular dynamics with NAMD. *J. Comput. Chem.* 26:1781–1802.
26. MacKerell, A. D., D. Bashford, …, M. Karplus. 1998. All-atom empirical potential for molecular modeling and dynamics studies of proteins. *J. Phys. Chem. B* 102:3586–3616.
27. Klauda, J. B., R. M. Venable, …, R. W. Pastor. 2010. Update of the CHARMM all-atom additive force field for lipids: validation on six lipid types. *J. Phys. Chem. B* 114:7830–7843.
28. Ryckaert, J. P., G. Ciccotti, and H. J. C. Berendsen. 1977. Numerical integration of the cartesian equations of motion of a system with constraints: molecular dynamics of *n*-alkanes. *J. Comput. Phys.* 23: 327–341.
29. Miyamoto, S., and P. A. Kollman. 1992. SETTLE: an analytical version of the SHAKE and RATTLE algorithm for rigid water models. *J. Comput. Chem.* 13:952–962.
30. Mintseris, J., B. Pierce, …, Z. Weng. 2007. Integrating statistical pair potentials into protein complex prediction. *Proteins* 69:511–520.
31. Kumar, S., D. Bouzida, …, J. M. Rosenberg. 1992. The weighted histogram analysis method for free-energy calculations on biomolecules. I. The method. *J. Comput. Chem.* 13:1011–1021.
32. Chen, R., A. Robinson, …, S. H. Chung. 2011. Modeling the binding of three toxins to the voltage-gated potassium channel (Kv1.3). *Biophys. J.* 101:2652–2660.
33. Carnevale, V., W. Treptow, and M. L. Klein. 2011. Sodium ion binding sites and hydration in the lumen of a bacterial ion channel from molecular dynamics simulations. *J. Phys. Chem. Lett.* 2:2504–2508.
34. Mills, J. E., and P. M. Dean. 1996. Three-dimensional hydrogen-bond geometry and probability information from a crystal survey. *J. Comput. Aided Mol. Des.* 10:607–622.
35. Garcia, M. L., Y. Gao, …, G. J. Kaczorowski. 2001. Potassium channels: from scorpion venoms to high-resolution structure. *Toxicon* 39:739–748.
36. Wilson, M. J., D. Yoshikami, …, M. M. Zhang. 2011. μ-Conotoxins that differentially block sodium channels $Na_V1.1$ through 1.8 identify those responsible for action potentials in sciatic nerve. *Proc. Natl. Acad. Sci. USA* 108:10302–10307.
37. Cummins, T. R., F. Aglieco, and S. D. Dib-Hajj. 2002. Critical molecular determinants of voltage-gated sodium channel sensitivity to μ-conotoxins GIIIA/B. *Mol. Pharmacol.* 61:1192–1201.
38. Humphrey, W., A. Dalke, and K. Schulten. 1996. VMD: visual molecular dynamics. *J. Mol. Graph.* 14:33–38, 27–28.